The application of reactive ion etching in producing free-standing microstructures and its effects on low-temperature electrical transport

Y. K. Kwong, K. Lin, P. Hakonen,[a] J. M. Parpia, and M. Isaacson
School of Applied and Engineering Physics and the Department of Physics, Clark Hall, Cornell University, Ithaca, New York 14853

(Received 30 May 1989; accepted 26 July 1989)

We have developed a reliable method of fabricating free-standing metallic microstructures with dimensions down to 50 nm. This technique is compatible with virtually any metal and can be used to fabricate samples that should be low-dimensional with respect to both electron and phonon transport. Unlike earlier schemes that effect substrate removal from the front, our technique calls for reactive-ion etching (RIE) from the reverse side of a Si_3N_4 membrane substrate, onto which microstructures have been previously patterned by standard methods. By carefully controlling the etching times, the extent of invasive damage of the etch on the microstructures is minimized. We have also performed resistance measurements for etched and unetched Al films on bulk substrates to characterize the effect of etching damage and its consequence on low-temperature transport. By measuring the low-field magnetoresistance (MR), the inelastic scattering rate and its dependence on temperature can be determined by fitting data to theoretical models. For short etch times, we have found that RIE does not alter the low-frequency electrical transport properties of these supported films in any significant fashion. The only discernible difference between the etched and the unetched samples appears to be a small, temperature-independent contribution to the inelastic rates, which can be attributed to surface damage. Thus, we conclude that our technique can be used to effectively decouple microstructures from substrate effects without introducing appreciable process related artifacts.

I. INTRODUCTION

Quantum transport in thin metallic films and wires has been studied extensively in the past decade.[1,2] Due to fabrication requirements, most work has necessarily been carried out on bulk substrates. Although this is adequate for probing quantum effects in electron transport, it is unsuitable for low-dimensional phonon studies. Santhanam *et al.*[3] showed that for clean Al thin films, the inelastic scattering rate for weak localization τ_{in}^{-1} as a function of the absolute temperature T, obeys the power law $AT + BT^3$. The linear term was attributed to two-dimensional electron–electron scattering and the cubic term to three-dimensional electron-phonon scattering. Experiments with thin wires by Wind *et al.*[4] gave $\tau_{in}^{-1} \sim AT^{2/3} + BT^3$, which was attributed to one-dimensional electron-electron scattering and, again, three-dimensional electron-phonon scattering. In short, electron-phonon processes are typically dominated by bulk phonons emanating from within the supporting substrate.

The relevant dimensionality for phonon dynamics is determined by the dominant phonon wavelength λ_{ph}. At low temperature, we can estimate this value by $\lambda_{ph} = \theta_D\, a/2T$, where θ_D is the Debye temperature and a is the lattice constant. For Al, $\theta_D \sim 400$ K and $a \sim 0.4$ nm, so $\lambda_{ph} \sim 80$ nm at 1 K. With modern fabrication technology, metallic samples with one or two physical dimensions smaller than this value can be readily fabricated. Thus, phonon dimensionality effects should be observable provided that the coupling of phonons between the microstructure and the substrate is small.

Different techniques can, in principle, be used to isolate thin metal films or wires from bulk phonons. In the literature, we have found four potentially workable approaches. First, unsupported thin films of different materials have been prepared by techniques involving the removal of thin films from crystalline salt substrates and transferring them to fine metal grids. These techniques have been used successfully to prepare samples for optical experiments[5] and electron microscopy.[6] However, they do not appear to be applicable to electrical measurements, as contacts cannot be easily made. Second, small Bi whiskers and Pt wires have been prepared by special growth or drawing methods.[7,8] These methods are nonstandard from the point-of-view of microfabrication. The transport data obtained in these studies are not fully understood since they do not conform to the standard theories of weak localization and Coulomb interaction. This is presumably due to artifacts of the sample preparation schemes. Third, Be thin films were evaporated onto mica substrates.[9] By relying on the acoustic mismatch between Be and mica, effects attributed to the reduction of phonon dimensionality were, in fact, observed in this study. However, this technique does not appear to have universal applicability since phonon coupling between metals and substrates is not small and, in any case, difficult to characterize. Fourth, free-standing wires were made using standard microfabrication methods by Smith *et al.*[10] In these studies, wires of $Au_{60}Pd_{40}$ were patterned by electron–beam lithography and liftoff, on a substrate of Si_3N_4 on bulk Si. Plasma etching was then performed, using a CF_4 plasma from the side with the metal wires. After typical etching times on the order of several minutes, the region of Si_3N_4 and Si supporting the wires was removed, leaving the wires free standing. The etching step was harsh and may have resulted in significant damage to the wires. Many wires were broken and the

 © 1989 American Vacuum Society

resistance per wire also increased significantly. It was difficult to differentiate etching damage from phonon dimensionality effects, if present at all.

We present here a technique inspired by the work of Smith *et al.*, but one which gives rise to considerably less damage to the microstructures. Our technique calls for reactive-ion etching (RIE) from behind a self-supporting Si_3N_4 membrane substrate on which microstructures have been patterned. Further, we address directly the issue of RIE-induced damage and its consequence on low-temperature transport. Specifically, low frequency resistance measurements were performed for two-dimensional Al microstructures on bulk substrates exposed to the identical RIE environment used to fabricate free-standing samples. Etching times were chosen to simulate reasonable RIE/microstructure interaction times during the preparation of free-standing structures. This study permits us to isolate the effects of the etching step. This, in turn, will permit us to assess RIE processing artifacts that may be produced when fabricating free-standing microstructures.

II. FABRICATION METHOD

All fabrication work was performed at the National Nanofabrication Facility at Cornell. Figure 1 outlines the fabrication steps. A self-supporting Si_3N_4 membrane was made by photolithographic patterning one side of a double-polished Si ⟨100⟩ wafer, followed by a KOH wet etch. To define metal microstructures on the nitride membrane and surrounding regions, standard photo- or electron-beam lithography, vapor-deposition, and liftoff processes were used. The supported microstructures were then made free-standing by RIE removal of the membrane from the backside, using the following process parameters: CHF_3/O_2 plasma at 30/1 sccm, 0.15 W/cm^2, and 30 mTorr. The typical time required to completely etch through the 140 nm nitride membrane is ~3.5 min.

Etching from the backside was achieved by simply placing the samples face down in the RIE chamber. After about 2.5 min, etching is continued in steps of 10 s, with cooling intervals of at least 3 min between steps. By frequent inspection of the samples between steps (under an optical microscope), the plasma/microstructure interaction time is limited to less than 20 s. The use of this incremental etching procedure prevents overheating of the samples, which may warp or even break the fragile free-standing structures.

Free-standing structures of Al, Ag, Au, and Cu have been successfully fabricated by this method. We expect this method to be compatible with virtually any material that can be vapor-deposited. Micrographs of typical two-dimensional and one-dimensional samples are shown in Figs. 2 and 3, respectively.

The wafer containing free-standing structures was scribed to yield (3 mm)^2 samples. Each sample was glued onto a copper header and electrical connections were made using an ultrasonic bonder. The bonded header was then mounted in a 1 K-cryostat to determine basic sample parameters.

We have examined two-dimensional Al samples, as shown in Fig. 2, from numerous batches. The residual resistance ratio (RRR) and the superconducting transition temperature T_c were determined. RRR was taken to be the ratio of the resistance at room temperature to that at 4.2 K. T_c was obtained by plotting the inverse of the fluctuation conductivity of a sample against T and extrapolating smoothly to the T-axis.[11] (We found that T_c obtained in this fashion agrees with the half-resistance point to within 2 mK.) The sheet resistance R_s at room temperature was also independently measured with a four-point probe on co-deposited films. R_s

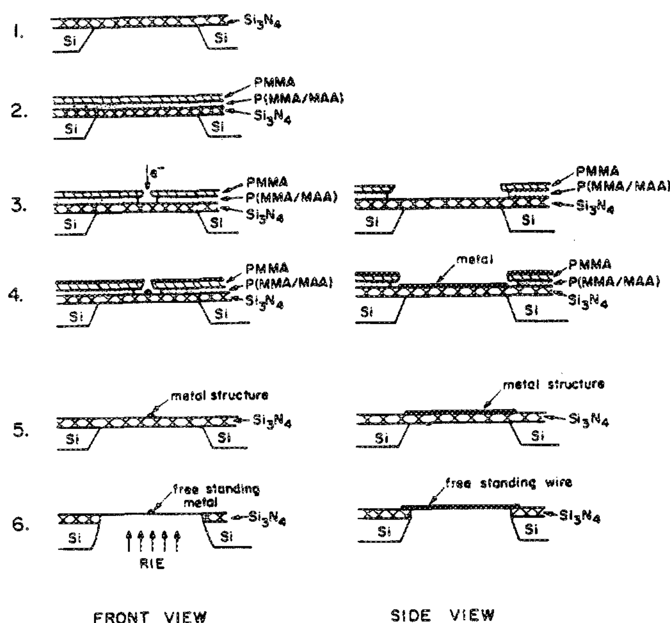

FIG. 1. Schematic of the fabrication scheme to produce free-standing microstructures. Step 1: Wet etch produces 140 nm thick Si_3N_4 membrane. Step 2: Resist is spun onto Si_3N_4 membrane. Step 3: Electron beam lithography and development. This step is photolithography when fabricating larger features. Step 4: Vapor-deposition of thin film. Step 5: Liftoff produces metal microstructures. Step 6: RIE removes Si_3N_4 membrane substrate.

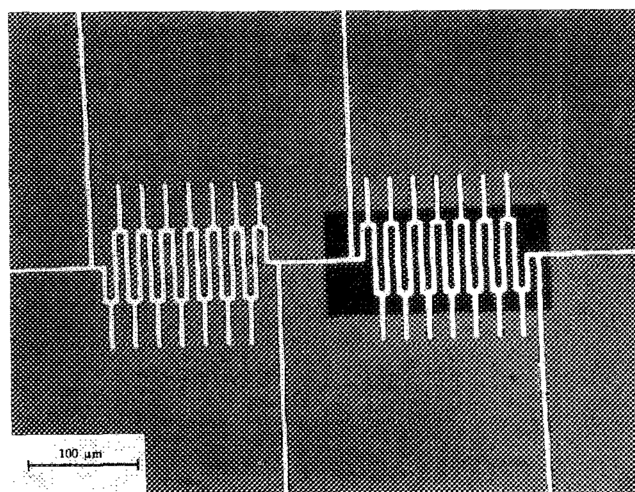

FIG. 2. Typical free-standing (right meander) Al film with contiguous supported section (left meander). The fingerlike projections are mechanical supports for the free-standing part of the current path. Defined by photolithography, these samples are suitable for four-point resistance measurements. Line width shown here is ~5 μm.

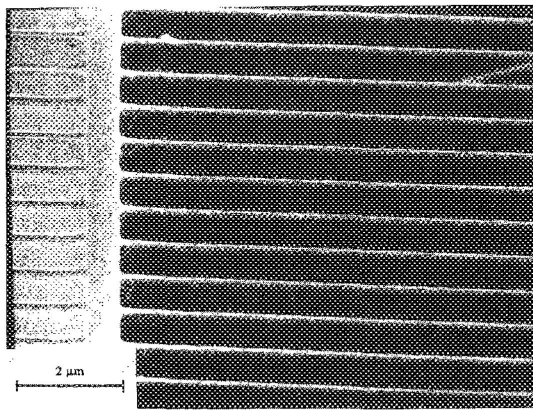

FIG. 3. Free-standing Au wires defined by electron-beam lithography. Line width shown here is ~150 nm, though we have fabricated wires down to 50 nm width reproducibly.

at 4.2 K was then taken as R_s at room temperature divided by RRR.

Depending on deposition conditions, RRR, T_c, and R_s may vary appreciably from batch to batch. However, values of RRR and T_c for contiguous supported and free-standing films on the same sample are generally very similar. Independent of batch, RRR for the supported and free-standing films are usually less than 1% different, but there is a slight suppression of T_c for the free-standing part with respect to the supported part. This suppression generally ranges from 30 to 50 mK from batch to batch. We speculate that it is the result of differential stress, which has been found to alter the T_c of Al.[12]

Before initiating detailed measurements on free-standing structures, we believe it is crucial that etching damage be carefully characterized, at least as far as its effect on transport is concerned. The similar RRR's of the supported and free-standing films suggest that etching damage is likely a small effect. However, as previous work on phonon dimensionality effects were almost always obscured by sample preparation artifacts, we have decided to undertake a more comprehensive etching study.

III. ETCHING DAMAGE STUDY

The application of RIE from the backside of a membrane substrate is expected to minimize damage to the microstructures. However, when the plasma etches through the nitride window, some interaction between the plasma and the microstructure cannot be avoided, and some degree of over-etch is inevitable. With careful techniques, this over-etch time can be limited to less than 20 s, with small variations from batch to batch.

A. Samples

For the etching study, we have prepared 25 nm thick, 5 μm wide Al microstructures on bulk Si_3N_4/Si wafers. An array of two contiguous meander patterns was defined by photolithograhy, vapor deposition, and liftoff as described above. Appropriate interconnects and bonding pads suitable for four-point resistance measurements were also patterned. The resultant structures are identical to those shown in Fig. 2 except all features reside on bulk substrate.

The wafer was then coated again with photoresist. Rectangular regions were photolithographically defined so that, upon development, one of the two contiguous meander patterns would become unmasked on each sample. To ensure that no resist residue remains on the rectangular openings, an O_2 plasma descum was performed for 10 s. The wafer was then returned to the RIE chamber and subjected to a CHF_3/O_2 plasma. Etching times of 10, 20, or 30 s were used, simulating a reasonable range of over-etch times when fabricating free-standing samples. The wafer was then rinsed in acetone to remove all undeveloped resist and scribed into $(3\ mm)^2$ samples. Aside from the O_2 descum step, these steps exactly mimic typical conditions during the preparation of free-standing structures.

B. Transport measurements

RRR, T_c, and R_s were determined as described in the last section. The electron diffusion constant D was determined by the change in the upper critical field close to T_c.[13] Low-field MR at various temperatures were also measured. When collecting MR data, the magnetic field was typically scanned from -100 to 400 G, with ~1 G increments close to zero field. An excitation current of 0.3 μA was used for measurements near T_c, and 3 μA for MR measurements. By checking reproducibility of data at lower currents, we have ascertained that no self-heating occurs at these excitation levels.

The resistance of a calibrated carbon-glass resistor was monitored for thermometry. With a heater under computer control, a temperature stability better than 0.5 mK was routinely achieved.

C. Results

The values of RRR and T_c for the unetched, or masked, sections of all samples studied are the same and are given in the first row of Table I. At several temperatures, we also found that MR data for the unetched sections of all samples to be virtually indistinguishable. The values of D were found to be nearly the same as well. (In fact, for both the unetched and the etched parts of the various samples used in this study, we found $D \sim 25\ cm^2\ s^{-1}$. This value is reproducible to within 10% and will be used in subsequent data analysis.)

TABLE I. Electrical properties of samples used in the etching damage study. RRR = $R(300\ K)/R(4.2\ K)$; T_c is determined as described in the text; and $R_s(4.2\ K) = R_s(300\ K)/RRR$.

Sample	RRR	T_c (K)	R_s (Ω) 4.2 K
Unetched	1.605	1.448	2.3
O_2 descumed only	1.586	1.488	2.3
10 s etched	1.599	1.469	2.3
20 s etched	1.599	1.475	2.3
30 s etched	1.613	1.478	2.3

As all samples were vapor-deposited as a single batch, these observations are not surprising and are further indication of the noninvasive property of the overall fabrication process.

The values of RRR and T_c for the etched parts of various samples are also shown in Table I. We observed good agreement ($\pm \sim 1\%$) of the RRR among all etched samples. In fact, within uncertainties, RRR for the etched and the unetched parts is the same. However, T_c is higher (20 to 40 mK) in the etched part than in its contiguous unetched part. As the T_c elevation is present even for the sample with O_2 descum only, we attribute this effect to the descum step. (We note that T_c elevation of Al with increasing oxidation has been well documented in the literature.[14]) Our data also suggest a slight increase of T_c with increasing CHF_3/O_2 RIE time. However, this effect may be due to variations in the O_2 descum time.

It is, by now, a standard practice to extract inelastic scattering rates, τ_{in}^{-1}, from MR data.[2] Following Gordon & Goldman,[11] we have fitted MR data for etched and unetched films to the theories of superconductivity fluctuations and localization. For known values of R_s, T_c, D, and the spin-orbit scattering rate τ_{so}^{-1}, a single parameter fit can be performed to obtain τ_{in}^{-1}. In this work, R_s, T_c, and D were determined experimentally. τ_{so}^{-1} was obtained by using a two-parameter fit for τ_{so}^{-1} and τ_{in}^{-1} at higher temperatures, where MR is more sensitive to τ_{so}^{-1}. The same value of τ_{so}^{-1} was then used for all temperatures, as it is expected to be temperature independent. We should point out that even though the values of τ_{so}^{-1} and D may have significant uncertainties, they do not affect the important qualitative features of τ_{in}^{-1} substantially. To minimize subjectivity in the fitting procedure, a simplex algorithm using a subroutine supplied by IMSL[15] was used to minimize the least-square deviations of the fit. Agreement between fits and data is usually excellent.

The result of this analysis is shown in Fig. 4, which shows τ_{in}^{-1} versus T for the different samples. At fixed T, τ_{in}^{-1} appears insensitive to RIE within the range of etching times chosen. (For clarity, the result for the 10 s sample is omitted. Within experimental errors, this curve would trace over those at other etching times.) This fact was actually obvious without any elaborate fitting, as MR data for all etched samples are practically indistinguishable. Values of τ_{in}^{-1} for the etched and unetched samples are also very similar, in absolute terms as well as temperature–dependence. Aside from a relatively small temperature-independent shift of about 0.8×10^8 s^{-1}, τ_{in}^{-1} for the etched sections is identical to the unetched sections. As τ_{in}^{-1} appears to be insensitive to CHF_3/O_2 etching time and is present even for O_2 descum only, we attribute this small shift in τ_{in}^{-1} to surface damage caused by the descum step.

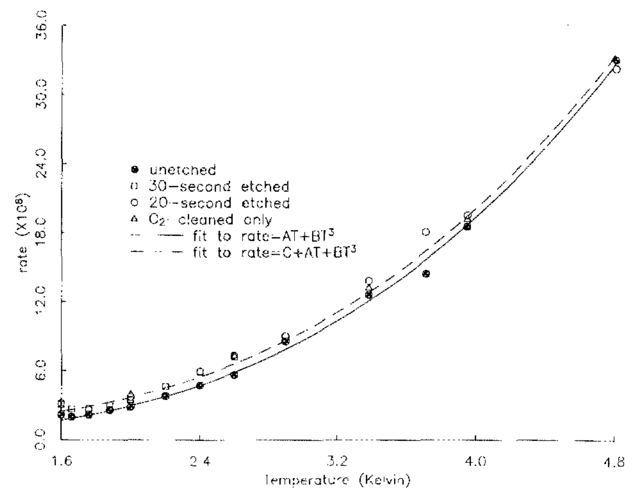

FIG. 4. Inelastic scattering rate τ_{in}^{-1} versus T. Note that both the etched (including the sample with O_2 descum only) and the unetched samples can be fitted to the same power law. Shown here, $A = 0.347 \times 10^8$, $B = 0.282 \times 10^8$, and $C = 0.75 \times 10^8$.

IV. CONCLUSION

Aside from small changes in T_c and τ_{in}^{-1} due to the O_2 descum step, the effect of etching damage on low-frequency electrical transport is insignificant. From the point of view of producing free-standing structures, these changes are not especially important, because no analogous descum step is required. We therefore conclude that the present technique is suitable for preparing free-standing samples in transport studies.

Some limitations of the current study should be pointed out. First, the surface-to-volume ratio in one-dimensional wires is higher than two-dimensional samples. (Our study has focused only on the latter.) For one-dimensional systems, we are hopeful that surface damage could be likewise minimized by carefully controlling the over-etch time. Second, the current study deals only with Al structures. For fixed over-etch time, the physical interaction between plasma of a fixed energy density and metals are not expected to be appreciably different across the Periodic Table. For RIE, physical damage should be small. Chemical damage should be small as well, since the reactivity between ions in a CHF_3 plasma and metals is, in general, weak. However, these assertions are somewhat speculative. For the sake of careful controls, similar etching damage studies should be performed when switching to the one-dimensional regime or to different materials. Finally, we have used a small concentration of O_2 when etching Si_3N_4. This is actually unnecessary. Since we have found that O_2 plasma may give rise to unwanted effects, its use should be eliminated in future work.

ACKNOWLEDGMENTS

The authors thank J. DiTusa, M. N. Wybourne, and R. A. Buhrman for helpful discussions. This work was partially supported by the AFOSR under AFOSR-87-0148, the Cornell Materials Science Center under DMR85-16616, and a grant from Tektronix, Inc. Work at the Cornell National Nanofabrication Facility was supported through NSF grant ECS-8619049. Y. K. K. was a G. E. Foundation Fellow during part of this project. K. L. was an I. B. M. Manufacturing Fellow.

[a] Current address: Low Temperature Laboratory, Helsinki University of Technology, Otakaari 3A, SF-02150 Espoo, Finland.

[1]B. L. Al'tshuler, A. G. Aronov, M. E. Gershenson, and Y. V. Sharvin, Sov. Sci. Rev. **9**, 223 (1987).
[2]G. Bergmann, Phys. Reports **107**(1), 1 (1984).
[3]P. Santhanum, S. Wind, and D. E. Prober, Phys. Rev. B. **35**(7), 3188 (1987).
[4]S. Wind, M. J. Rooks, V. Chandrasekhar, and D. E. Prober, Phys. Rev. Lett. **57**, 633 (1986).
[5]M. Grimsditch, R. Bhadra, and I. K. Schuller, Phys. Rev. Lett. **58**(12), 1216 (1987).
[6]For example, see *Techniques for Electron Microscopy*, 2nd ed., edited by D. Kay (Blackwell, Oxford, 1965).
[7]D. R. Overcash, B. A. Ratman, M. J. Skove, and E. P. Stillwell, Phys. Rev. Lett. **44**(20), 1348 (1980).
[8]A. C. Sacharoff, R. M. Westervelt, and J. Bevk, Phys. Rev. B **29**(4), 1647 (1984).
[9]A. V. Butenko, E. I. Bukhshtab, V. Yu. Kashivin, and Yu. F. Kamnik, Sov. J. Low Temp. Phys. **14**(4), 233 (1988).
[10]C. G. Smith, H. Ahmed, and M. N. Wybourne, J. Vac. Sci. Technol. B 5(1), 314 (1987). C. G. Smith and M. N. Wybourne, Solid State Commun. **57**(6), 411 (1986).
[11]J. M. Gordon and A. M. Goldman, Phys. Rev. B **34**(3), 1500 (1986). See also B. Shinozaki, T. Kawaguti, and Y. Fujimori, J. Phys. Soc. Japan **55**(7), 2364 (1986).
[12]D. R. Overcash, T. Davis, J. W. Cook, Jr., and M. J. Skove, Phys. Rev. Lett. **46**(4), 287 (1981).
[13]M. Tinkham, *Introduction to Superconductivity* (McGraw-Hill, New York, 1976).
[14]For example, see B. Abeles, R. W. Cohen, and G. W. Cullen, Phys. Rev. Lett. **17**, 632 (1966).
[15]IMSL MATH/Library of FORTRAN Subroutines, Edition 10.0, Houstion: IMSL (1987).